PERGAMON

Chemical Engineering Science 58 (2003) 1687–1701

Chemical Engineering Science

www.elsevier.com/locate/ces

Consolidation dewatering and centrifugal sedimentation of flocculated activated sludge

S. J. Lee[a], C. P. Chu[a], R. B. H. Tan[b], C. H. Wang[a,b], D. J. Lee[a,*]

[a] *Department of Chemical Engineering, National Taiwan University, 1, Sec. 4 Roosevelt Road, Taipei 10617, Taiwan*
[b] *Department of Chemical and Environmental Engineering, National University of Singapore, 4 Engineering Drive 4, Singapore 117576, Singapore*

Received 28 June 2002; received in revised form 19 September 2002; accepted 24 December 2002

Abstract

This study investigated experimentally the consolidation dewatering and centrifugal-settling processes for activated sludge subjected to cationic polyelectrolyte flocculation. The results were reported for the dynamic response of sediment cake thickness (an index for cake compaction) under various doses of polyelectrolyte conditioning, compression–permeability cell configuration and mode of operation (batch and continuous) in a centrifugal-settling cell. The reduction in sediment thickness of sludge by consolidation and centrifugation was found to correspond mostly well with the optimal dose of polyelectrolyte based on the capillary suction time. The relaxation/rebound of cake thickness was observed in both consolidation dewatering and centrifugal dewatering with comparable compaction/relaxation time scale ratios. The equilibrium sediment consolidation ratio increases with the effective solid pressure characterized by P_m and P_s, for the consolidation dewatering and centrifugal sedimentation, respectively. The experimentally determined time scales of the cake consolidation dewatering/centrifugal sedimentation processes agree reasonably well with the theory by Landman and Russel (Phys. Fluids A 5 (1993) 550).

Keywords: Cake; Consolidation; C–P cell; Centrifugal settling; Plastic deformation,

1. Introduction

Multistage consolidation/centrifugation dewatering is sometimes encountered in wastewater treatment processes. In order to achieve smooth function in such devices, it is important to have fundamental understanding of these individual unit operations for solid/liquid separation applications.

Buscall and White (1987) investigated the consolidation of concentrated suspensions and proposed a theory of sedimentation. Their analysis considered empirical yield stresses for the network of flocculated suspensions which need to be determined by further studies. In calculating the initial sedimentation rate under uniform acceleration, a method had been proposed to estimate the compressive yield stress from centrifuge experiments. Subsequently, the basic concept was further extended via a series of studies by Landman and workers (Landman & Russel, 1993; Landman, White, & Eberl, 1995; de Kretser et al., 2001) to investigate the pressure filtration of flocculated suspensions. Landman and Russel (1993) used a power-law expression (to relate the empirical yield stress with local solid volume fraction) in a one-dimensional model for a pressure filter and examined the relative magnitudes of the time scales for filtration and sedimentation. Later, Landman et al. (1995) considered the pressure filtration of flocculated suspensions by various types of rheological power-law functions for the compressive yield stresses. The resulting similarity solution for consolidation stage agreed reasonably well with conventional engineering analysis of the same problem which correlates consolidation ratio with consolidation date by an empirical formula.

Results about the consolidation dewatering in compression–permeability (C–P) cells have been reported in the literature (Lu, Huang, & Hwang, 1998; Wu, Lee, Zhao, Wang, & Tan, 2000; Wu, Lee, Wang, Chen, & Tan, 2001). It is usually assumed that the dependence of compressive stress on the local volume fraction in the cake can be determined through such a device. In general, sidewall friction constitutes a significant fraction of the total pressure transmitted throughout the filter cake. Under such conditions, the

* Corresponding author. Tel.: +886-223625632; fax: +886-22362-3040.
E-mail address: djlee@ccms.ntu.edu.tw (D. J. Lee).

0009-2509/03/$ - see front matter © 2003 Elsevier Science Ltd. All rights reserved.
doi:10.1016/S0009-2509(03)00020-4

deviation of porosity distribution from a one-dimensional cake structure is expected.

Centrifugal dewatering/settling processes using polyelectrolyte flocculents have commonly been seen in wastewater treatment plants. Chu and Lee (2001) showed that sludge flocculation would yield a significant sedimentation effect at the first stage. They observed that an optimal rotational speed exists to which the dewatering rate reaches a maximum. Yen and Lee (2001) showed that the plastic deformation is observed in the centrifugal-settling method. For instance, the irreversible yielding in activated sludge cake formed under 200–500 rpm centrifugation (equivalent to 8–50g acceleration) can result in higher than 25% error in the estimation of bound water content. The error is made due to the fact that subjected to the removal of centrifugal force, the sediment rebounds corresponding to over 25% rebound ratio.

Most of the above analyses were focused on one-step consolidation dewatering or centrifugal-settling processes. Multistage processes have not been the main topic of research until recently. Usher, de Kretser, and Scales (2001) proposed a new technique for dewatering characterization based on stepped pressure filtration compressibility and permeability tests to determine $P_y(\varphi)$ and hindered settling function $R(\varphi)$. The results were analyzed with a set of key filtration equations using the pressure filtration theories developed by Landman and colleagues (Landman & Russel, 1993; Landman et al., 1995).

In view of the progress of the previous studies mentioned above, the objectives of the present study are three-fold: (i) quantitative comparison of the dewaterability of a wet cake by consolidation and centrifugal settling; (ii) understanding the difference in efficiency between the dewaterability of continuous and batch stepped operations; (iii) determining the relaxation of the wet cake subject to the release of external driving forces (consolidation pressure, rotational torque) and its implication on the elastic/plastic deformations of the cake.

2. Material and methods

2.1. The sample

Sample-U: Activated sludge samples (pH 6.8–7.1) were taken from the reflux stream of Ulu Pandan Sewage Treatment Works, Singapore. The design of the Works is based on conventional activated sludge process using diffused air aeration system, having a total treatment capacity of 361000 m^3/day. After thickening, the dry solid content of sludge, determined by weighing and drying at 104°C, was 1.33% w/w. The chemical oxygen demand for the supernatant (COD) and that for the total sludge (TCOD) are 103 and 8500 mg/l, respectively. After the mixing and prior to the settling, a small quantity of sludge–polymer aggregates in the vessel was transferred carefully into the fresh electrolyte at the same pH and electrolyte concentration as the original Sample-U and T.

Sample-T: Activated sludge was taken from the wastewater treatment plant in Presidential Bread Plant (Chung-Li, Taiwan) which treats approximately 250 ton of food processing wastewater per day using conventional activated sludge process. The sample was taken from the recycled sludge stream, whose sediment was the testing sample with a solid weight percent of 0.7% w/w.

2.2. Capillary suction time (CST) and cationic polyelectrolyte conditioning

Capillary suction apparatus as described in Lee and Hsu (1992, 1993) was employed to estimate the sludge filterability. In brief, the inner cylinder radius was 0.535 cm. The time required for the filtrate to migrate from 1.5 to 3.0 cm was defined as the CST. The sludge was subject to chemical or physical conditioning. For chemical conditioning, the cationic polyelectrolyte indicated as polymer T-3052 was obtained from Kai-Guan Inc., Taiwan. The polymer T-3052 is a polyacrylamide with an average molecular weight of 10^7, and a charge density of 20%.

2.3. Light scattering tests

Small-angle laser light scattering tests were conducted using a Malvern Mastersizer/E which consists of a 5 mW He–Ne laser ($\lambda = 632.8$ nm) as the light source, and an optic lens and photo-sensitive detectors. The scattered light was collected at angles between 0.03° and 6.52° using a 31-element solid-state detector array. The light obscuration level of samples had to be maintained between 10% and 30% for reliable measurements. The Malvern Mastersizer/E was also used to measure the aggregate size between 1.2 and 600 μm. The Mastersizer measures the scattered light 20 times, each time for 20 s, over a total of 400 s. A small magnetic stirrer was installed in the scattering chamber to suspend the sample particles. The induced current did not markedly affect the scattered intensity from samples. Such a stirrer is essential for reliable measurement, especially for flocculated sludge flocs whose sizes, which determine the sedimentation velocities, are generally large.

2.4. C–P cells

Figs. 1a and b depict the schematic diagrams of the C–P cells and other supportive apparatus proposed by Teoh, Tan, He and Tien (2001) (cell-S, located at the National University of Singapore) and by Lu et al. (1998) (cell-T, located at the National Taiwan University). The load at the top and the transmitted pressure to the bottom surface were measured together with the cake height during each test. The cell-S had a cylinder made of stainless steel with inner diameter 75.3 mm. The cylinder of cell-T was made

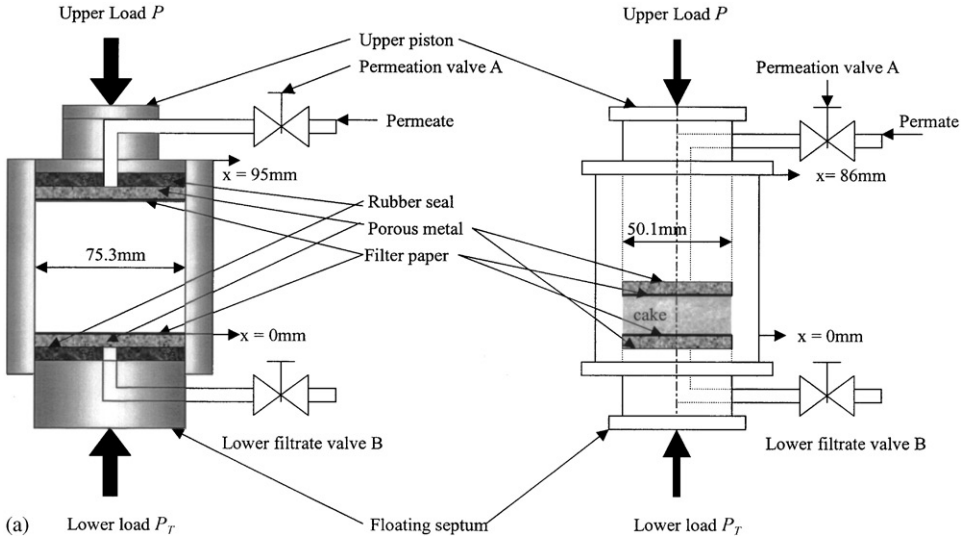

Fig. 1. Schematic diagram of the (a) C–P cell (cell-S) and (b) C–P cell (cell-T).

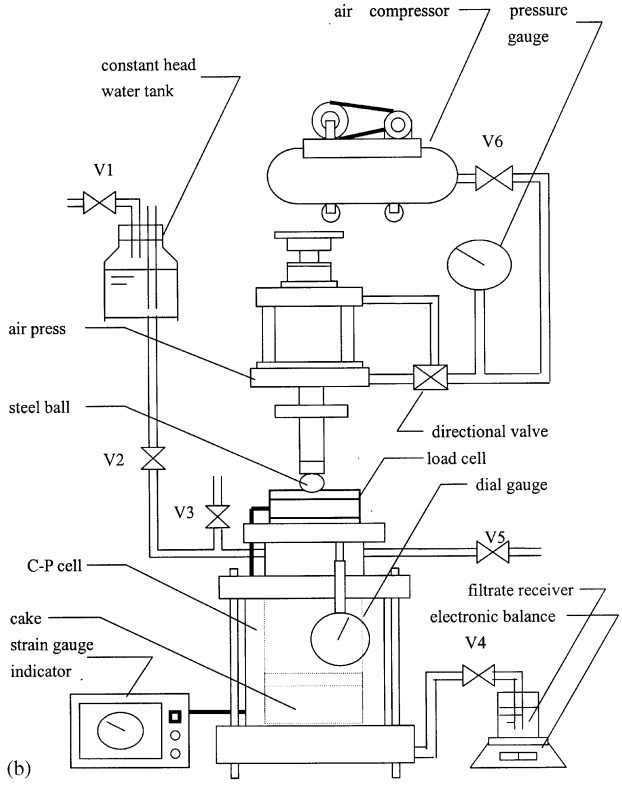

Fig. 1. *continued.*

of acrylate which has an inner diameter of 50.1 mm. Based on the same cake height, the cake/cell wall contacting area was greater for cell-S than that for cell-T. The other details for these two apparatus could be found in Wu et al. (2000) and Lu et al. (1998), respectively.

Cell-S: The load at the top and the transmitted pressure to the bottom surface were measured together with the cake height during each test. A complete C–P cell test comprised two stages: the compression stage and the permeation stage. The cell could track both stages since all data from pressure transducers as well as from the displacement measurement were automatically sent to a computer for storage and processing. The pressure range under investigation was 25–200 kPa. The choice of such a pressure range for test was attributed the following two reasons. Firstly, in preliminary tests at the applied pressure of 50 kPa the cake structure of activated sludge revealed a significant collapse, which had not occurred at the test of the less pressure. Hence the lower limit for applied pressure under investigation was set at 25 kPa. Moreover, since the total testing time had to be limited within 7 days, the upper pressure limit was taken as 200 kPa. Although the practical range for sludge dewatering could be up to 500–700 kPa, however as the present experimental data illustrate, the basic characteristics for cake properties would keep unchanged at pressures exceeding 200 kPa.

Cell-T: For the sake of comparison, all experimental conditions were maintained to be closely similar to cell-S, including slurry preparation as well as the subsequent calibration and data acquisition. After the compression having reached equilibrium under the applied load, the thickness of compressed cake was measured and recorded. The pressure range under investigation is 13–202 kPa.

2.5. Consolidation–relaxation experiments

Prior to the C–P cell test the septum was first filled with filtrate. The slurry was carefully poured into the cylinder and drained to form a saturated, wet cake. The piston was positioned at the top of formed cake, through which the mechanical force was applied. During the compression the valve-A (permeation valve) was close and valve-B open,

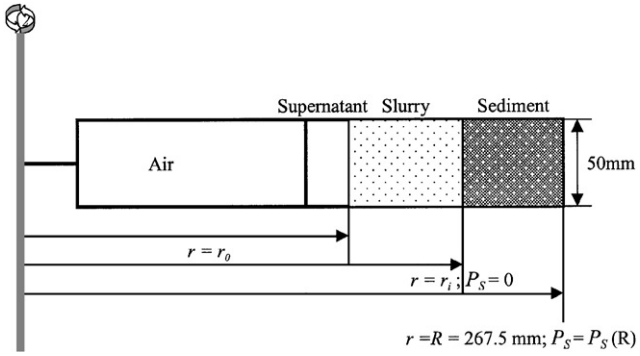

Fig. 2. Schematic illustration of the centrifugal tests. P_s: local solid compressive pressure of the centrifugal test (Pa); R: distance between center of centrifuge and bottom of sediment (m); r: radial coordinate of cylindrical coordinate system (m); r_i: distance from center of centrifuge to surface of sediment (m): Ω angular velocity of the centrifuge (rpm or rad/s).

which allowed the drainage of the filtrate. Before and after having reached mechanical equilibrium with the applied load, the thickness of compressed cake was continuously measured and recorded. Then the permeation test was conducted by allowing the filtrate to flow from a constant-head reservoir through the valve-A and the cake. An electronic balance measured the filtrate weight. With the flow rate and the pressure drop data, the specific resistance to filtration of cake could be determined. The temperatures during testing were used to correct the viscosity of filtrate.

The transmitted pressure at the bottom of the cake, P_t, was also recorded and compared with P. Consolidation–relaxation curve for testing sample-T (with four different doses of original, 80, 160, and 280 ppm, respectively) on the cell-T was constructed. Five panels of L/L_0 vs. time curves are shown in the consolidation plot with increasing axial loads (in the order of 13, 32, 49, 104, and 202 kPa). Each plot is followed by a relaxation curve during which the axial load was suddenly released to ambient pressure ($P = 0$), and then the cake thickness was recorded as a function of time.

Similarly, the consolidation–relaxation curve for testing sample-U on the S-cell was constructed for four different doses of original, 80, 280, and 480 ppm, respectively. Four panels of L/L_0 vs. time curves are shown in the consolidation plot with increasing axial loads (in the increasing order of $P = 25$, 50, 100, and 200 kPa).

2.6. Centrifugal-setting–relaxation experiments

The arm-suspended centrifuge proposed by Yen and Lee (2001) was modified and used in the present study. Fig. 2 shows a sediment of equilibrium thickness in a centrifugal tube. Transparent plastic chamber (with the inner diameter and length being 4 and 7 cm, respectively) was used for better visual observation. The setting cell was connected to a rotating arm. The length from the center of rotation to the filter medium and the span angle from the center of rotation to the filter medium were measured as 26.5 cm and 12°, respectively. A total of 97.4 g of sludge was put into the setting cell. The initial height of sample was 6.0 cm (L_0). A rotational speed ranging from 300 to 1050 rpm was regulated by a variable-speed motor through driving the motor belt. The effective one-dimensional centrifugal field, accelerating at the bottom of the cell of 27.4–336.2g, was analogous to the one-dimensional consolidation process mentioned in the proceeding section. A stroboscope emitting light synchronized with the rotating cell that "froze" the image of the supernatant–sediment interface of the centrifuged slurry. The corresponding images at different time steps were captured by a video camera. The stepwise change of rotation speed could be carried out in two different modes: batch mode and continuous mode. Centrifugal-settling experiments were carried out for testing Sample-T with four different doses of original, 80, 160, and 280 ppm. Three panels of L/L_0 vs. time curves were shown in the consolidation plot with increasing rotation speed (batch operation in the order of 300, 450, 550, 850 rpm). Each of these plots was followed by a relaxation curve in which the torque to the rotation speed was suddenly removed, and then the cake thickness was recorded as a function of time. Similar procedures were applied for Sample-U for four different doses: original, 80, 280, and 480 ppm, respectively. Four panels of L/L_0 vs. time curves were shown in the consolidation plot with continuous increasing rotation speed in the order of 350, 560 and 1050 rpm.

In the batch mode of operation, the preliminary tests showed that most of the sediments from Sample-T could reach mechanical equilibrium within 1500 s. Hence the centrifugal settling was recorded for 2000 s. The exceptional cases were for the original sludge and at low rotational speeds 300 and 450 rpm, under which conditions the mechanical equilibrium was established after about 3000 and 2000 s, respectively. In order to capture the complete dynamic behavior of the sediment cake, the corresponding record times were set as 4000 and 3000 s, respectively. The sludge height equilibrated with the centrifugal force was termed as L_c. Subsequently, the centrifuge speed was reduced in 10 s till a complete stop. The sediment height was monitored continuously for another 600 s for the relaxation (rebound) of the sediment height. The final sediment height was termed as L_s. In the continuous mode of centrifugal-settling–relaxation experiments (Sample-U), the procedures were largely the same as the batch mode operation except that the increase of rotational speed was carried out in a stepwise way (350, 560 and 1050 rpm). As a result, the sediment formation followed a particle deposition pattern different from the batch mode operation. The time taken to reach equilibrium was in general more than 3000 s, much longer than the batch operation. The rebound of the sediment was recorded for about 800 s.

2.7. Comparison between consolidation dewatering and centrifugal-settling tests

The centrifugal acceleration can be related to the effective radial pressure gradient across the sediment/cake by the following formula (Lee, 1994; Chu & Lee, 2001):

$$\frac{\partial P}{\partial r} = \frac{\partial P_L}{\partial r} = \rho_l r \Omega^2 \quad \text{at } r_0 < r < r_i, \tag{1}$$

$$\frac{\partial P}{\partial r} = \frac{\partial P_L}{\partial r} + \frac{\partial P_s}{\partial r} = \rho_l r \Omega^2 + (\rho_s - \rho_l)(1-\varepsilon) r \Omega^2 \quad \text{at } r_i < r < R, \tag{2}$$

where P_s is the local solid compressive stress, ε the local porosity of the sediment, ρ_s and ρ_l the density of the solid and liquid, and Ω the angular velocity of the centrifuge. For a given rotational speed Ω, one can use Eq. (2) to calculate the equivalent radial pressure gradient.

Integration of the solid pressure in Eq. (3) with respect to r yields the compressive stress at the bottom of the tube, $P_s(R)$ (Murase, Iwata, Adachi, Gmachowski, & Shirato, 1989):

$$P_s(R) = (\rho_s - \rho_l)\Omega^2 \int_{r_i}^{R} (1-\varepsilon) r \, \mathrm{d}r, \tag{3}$$

where r_i denotes the distance from center of centrifuge to surface of sediment. The reading of r_i is based on the average of triplicate sample measurements from three different locations. The error introduced in such averaging would not be significant when the ratio $(R-r_i)/R$ is much smaller than 1. If $R \gg R - r_i$, Eq. (3) could be approximated as follows:

$$P_s(R) = (\rho_s - \rho_l)\Omega^2 \frac{R + r_i}{2} \int_{r_i}^{R} (1-\varepsilon) \, \mathrm{d}r = (\rho_s - \rho_l)\Omega^2 \frac{R + r_i}{2} \omega_0, \tag{4}$$

where ω_0 refers to the total solid volume in the mixture per unit sectional area. Eq. (4) is then applied to Eq. (2) to evaluate the average radial pressure gradient across the cake:

$$\frac{\mathrm{d}P}{\mathrm{d}r} = \frac{\mathrm{d}P_L}{\mathrm{d}r} + \frac{\mathrm{d}P_s}{\mathrm{d}r} = \rho_L r \Omega^2 + \frac{P_s(R)}{(R - r_i)}. \tag{5}$$

In using Eq. (5) to calculate the radial pressure gradient, it is assumed that the solid compressive stress at the surface and bottom of the sediment is 0 (refer to Fig. 2) and $P_s(R)$, respectively. Table 1 lists the pressure gradient yielded in the centrifuge according to Eq. (5). From the tabulated values, it is seen that the predicated radial pressure gradient via Eq. (2) is about the same magnitude as with Eq. (5); the rotational speed 300–850 rpm (Sample-T) and 350–1050 rpm (Sample-U) correspond to the equivalent radial pressure of 0.239–1.940 and 0.326–2.961 MPa/m, respectively.

The analogy between the rotational speed and consolidation axial loads can be deduced by matching the radial pressure gradient. For a given axial load P, the effective axial pressure gradient across the cake is given by

$$\frac{\partial P}{\partial x} = \frac{P - P_t}{H}, \tag{6}$$

where H is the equilibrium thickness of the cake. Table 2 summarizes the values of axial pressure gradient ($\mathrm{d}P/\mathrm{d}x$) computed by Eq. (6). In one of the columns, the definition of log mean pressure difference (P_m) is given by the following:

$$P_m = \frac{P - P_t}{\ln(P/P_t)}. \tag{7}$$

The dependence of P_m on the porosity is found to agree reasonably well with a previous work (Wu et al., 2000).

2.8. Scanning electron microscopic photographs

The sludge flocs were first immersed in glutaraldehyde and followed in OsO_4 to chemically fix the components like protein and lipids. The moisture in the flocs was gradually replaced by raising-concentration alcohol (50%, 60%, 70%, 80%, 90%, 95%, and 100%) and acetone (100%). After critical point drying (CPD) (LADD) and coating by gold (SPISUPPLIES ION SUPTTER), the flocs were ready for SEM observation (JSM-5600, JEOL, Japan). The pre-treating procedure of sludge cakes was slightly different from the flocs. The dewatered cakes (from centrifuge or C–P cell) were first embedded in high-melting-point agarose to keep the entire shape. Some clump near the surface was taken away carefully and then immersed in the glutaraldehyde and OsO_4. The subsequent procedures were then completely the same as the sludge flocs. Agarose sticking on the cake (white portion) should be carefully removed to ensure the cake surface could be observed by electron beam.

3. Results and discussion

The relevant properties (CST, ζ-potential, and mean-mass -diameter) for Sample-T and Sample-U are summarized in Fig. 3. In general, the solution pH is within the range 6.7–7.1 and the specific gravity of the solution is around 1.4. An optimal dosage of sludge conditioner can be defined as either the amount of added chemicals that yields a distinct optimal dewaterability or the lowest amount of added chemicals that results in an acceptable dewatering performance (Christensen, Sorensen, Christensen, & Hansen, 1993). The optimal polyelectrolyte dose for the Sample-T and Sample-U was found to be 160 and 280 ppm, respectively (Fig. 3). The CST for original sludge was measured as 159 s (Sample-T) and 96 s (Sample-U). With the increasing doses of flocculent, the CST was reduced till the optimal dose point where the CST values read 25 and 22 s for the Sample-T and Sample-U, respectively.

Zeta (ζ-) potentials of aggregates were then measured by the zeta-meter (Zeter-Meter System 3.0, Zeter-Meter

Table 1
Equilibrium pressure gradient and yield stress on the sediment/cake in centrifugal-settling experiments

Ω (rpm)	Γ-value	L/L_0	ϕ_b (dimensionless)	P_s (Pa) (Eq. (4))	dP/dr (Pa/m) (Eq. (2))	dP/dr (Pa/m) (Eq. (5))	P_v ($\phi(0)$) (Pa) (Eq. (9))	$\phi(0)$ (Eq. (10))
Sample-T, original								
300	26.9g	0.500	0.0125	36.6	270,000	240,000	38.5	0.0139
450	60.6g	0.421	0.0128	82.7	609,000	539,000	88.9	0.0182
550	90.5g	0.400	0.0154	123.8	910,000	807,000	133	0.0212
850	216.3g	0.301	0.0234	300.0	2,180,000	1,940,000	304	0.0922
Sample-T, 80 *ppm*								
300	26.9g	0.523	0.0119	36.5	270,0000	240,000	38.4	0.0133
450	60.6g	0.417	0.0132	82.9	609,000	540,000	87.3	0.0187
550	90.5g	0.378	0.0163	124	911,000	807,000	131	0.0234
850	216.3g	0.289	0.0234	299	2,180,000	1,930,000	316	0.113
Sample-T, 160 *ppm*								
300	26.9g	0.497	0.0125	36.6	270,000	240,000	38.5	0.0138
450	60.6g	0.417	0.0132	83.0	609,000	540,000	87.4	0.0178
550	90.5g	0.423	0.0146	124	910,000	807,000	130	0.0188
850	216.3g	0.329	0.0210	299	2,180,000	1,940,000	309	0.0436
Sample-T, 280 *ppm*								
300	26.9g	0.473	0.0131	36.6	271,000	240,000	38.6	0.0144
450	60.6g	0.364	0.0154	83.1	610,000	542,000	86.2	0.0205
550	90.5g	0.296	0.0211	125.7	913,000	810,000	131	0.0283
850	216.3g	0.311	0.0225	298	2,180,000	1,940,000	303	0.0427
Sample-U, original								
350	36.7g	0.941	0.0098	61.3	381,000	326,000	63.3	0.0105
560	93.9g	0.928	0.0100	157	975,000	836,000	162	0.0114
1050	330.0g	0.675	0.0137	567	3,480,000	2,940,000	585	0.0259
Sample-U, 80 *ppm*								
350	36.7g	0.857	0.0108	61.8	382,000	327,000	63.8	0.0117
560	93.9g	0.617	0.0150	162	995,000	837,000	167	0.0183
1050	330.0g	0.498	0.0186	577	3,540,000	2,950,000	596	0.0549
Sample-U, 280 *ppm*								
350	36.7g	0.927	0.0100	61.4	368,000	326,000	63.4	0.0109
560	93.9g	0.826	0.0112	159	941,000	836,000	164	0.0136
1050	330.0g	0.534	0.0173	575	3,320,000	2,950,000	594	0.0801
Sample-U, 480 *ppm*								
350	36.7g	0.650	0.0145	63.3	368,000	328,000	64.0	0.0154
560	93.9g	0.543	0.0174	164	944,000	840,000	166	0.0203
1050	330.0g	0.400	0.0236	583	3,320,000	2,960,000	590	0.0642

Inc., USA). The results for original sludge flocs read −12.9 mV (Sample-U) and −19.5 mV (Sample-T). The readings for the flocculated sludge were in the range of −12.8 to −14.9 mV (Sample-T) and −8.43 to −15.3 mV (Sample-U). The particle size distribution was determined by Malvern Mastersizer/E with a mean-mass-diameter of approximately 151.9 μm and 68.7 mm for the Sample-U and Sample-T, respectively. The true solid density was measured by Accupyc Pycometer 1330 (Micromeritics), giving a measure of 1396.7 kg/m^3 (Sample-U) and 1450 kg/m^3 (Sample-T) with a relative deviation of less than 0.5%.

The consolidation tests on cell-T showed faster sludge dewatering for increasing doses of polyelectrolyte flocculation (Fig. 4). There was hardly any dewatering for all samples when the axial load P was kept below 13 kPa. When $P = 32$ kPa, the collapse of the sediment cake was observed for the samples with doses higher than 80 ppm. This was accompanied by the dewatering of about 50–60% of the total moisture contents in the conditioned sludge. In contrast, under the same level of axial load P, the dewatering of the original sludge was limited to only 10% of the total moisture contents. It was noted that the

Table 2
Equilibrium pressure gradient and yield stress on the sediment/cake in consolidation dewatering experiments

P (Pa)	P_t (Pa)	P_m (Pa)	ϕ_b(dimensionless)	H (mm)	dP/dx(Pa/m)
Sample-T, original					
14,000	2000	6160	0.0350	49.8	240,000
31,300	6000	15,300	0.0373	46.8	540,000
49,500	17,500	30,800	0.0467	37.4	858,000
107,000	71,500	88,100	0.0601	29.0	1,230,000
207,000	179,000	193,000	0.0758	23.0	1,210,000
Sample-T, 80 *ppm*					
15,300	2000	6540	0.0324	47.1	283,000
30,900	18,000	23,900	0.0670	22.8	569,000
47,600	27,000	36,300	0.0762	20.0	1,030,000
104,000	80,000	91,600	0.0990	15.4	1,580,000
207,000	175,000	191,000	0.123	12.4	2,590,000
Sample-T, 160 *ppm*					
13,000	1000	4680	0.0292	48.2	24,900
31,600	25,000	28,200	0.0746	18.9	349,000
47,600	37,000	42,100	0.0829	17.0	625,000
107,000	90,000	98,300	0.110	12.8	1,340,000
205,000	191,000	198,000	0.132	10.6	1,350,000
Sample-T, 280 *ppm*					
13,000	1000	4680	0.0403	42.9	280,000
30,900	20,000	25,100	0.102	17.0	646,000
49,500	40,500	44,800	0.116	15.0	604,000
105,000	72,500	87,800	0.156	11.1	2,950,000
205,000	186,000	195,000	0.196	8.85	2,180,000
Sample-U, original					
23,600	1200	7510	0.0267	49.9	449,000
49,400	2400	15,500	0.0511	26.1	1,800,000
98,800	44,300	68,000	0.0992	13.4	4,060,000
199,000	144,000	170,000	0.152	8.76	6,280,000
Sample-U, 80 *ppm*					
23,600	1200	7500	0.0366	36.4	616,000
49,400	4790	19,100	0.0755	17.6	2,530,000
98,800	45,500	68,800	0.122	11.0	4,870,000
199,000	141,000	168,000	0.216	6.17	9,300,000
Sample-U, 280 *ppm*					
23,600	1200	7500	0.0354	38.0	588,000
49,400	2400	15,500	0.0478	28.1	1,670,000
98,800	43,100	67,200	0.186	7.24	7,690,000
199,000	139,000	167,000	0.266	5.06	11,800,000
Sample-U, 480 *ppm*					
23,600	1200	7500	0.0360	37.5	597,000
49,400	7190	2190	0.115	11.7	3,610,000
98,800	5390	74,100	0.214	6.3	7,130,000
199,000	150,000	173,000	0.328	4.11	11,900,000

polyelectrolyte flocculation had improved significantly the dewatering capability under the same mechanical load range and the fastest consolidation dewatering occurred at 180 ppm, exceeding that with the CST estimated optimal polyelectrolyte dose (160 ppm in Fig. 3). Even at higher axial loads ($P = 49$, 104, 202 kPa), the decrease in the sediment thickness showed a monotonic decrease and dewatering was about 60–80% of the original moisture contents in the flocculated sludge. Within this range of axial load, the dewatering of the original sludge was much more significantly ranging from 30% to 50% of the original moisture contents.

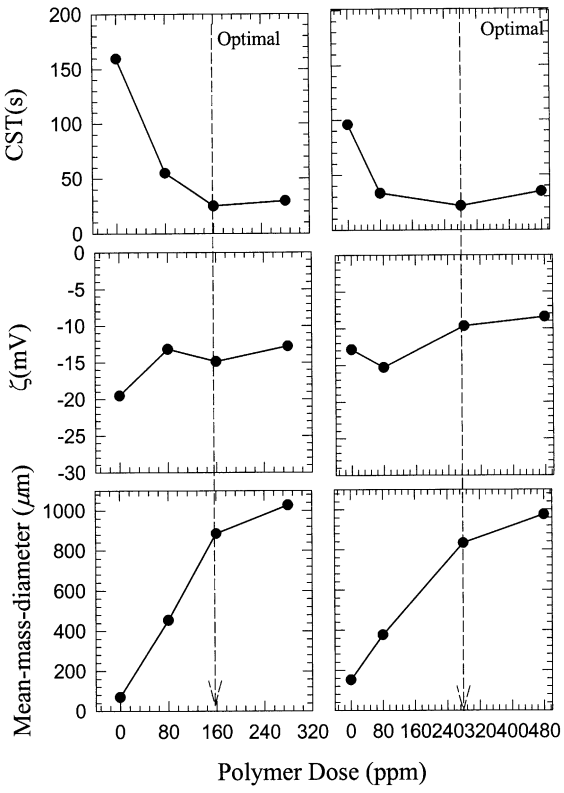

Fig. 3. Characteristics of Sample-T (left) and Sample-U (right) sludge before and after flocculation. Sample-T: pH=6.8, solid weight %=0.947%, density = 1450 kg/m^3. Sample-U: pH = 6.8–7.1, solid weight % = 1.33%, density = 1397 kg/m^3.

The capillary suction pressure in CST test is commonly estimated around 15 kPa (Lee & Hsu, 1992; Lin & Lee, 2001). This low pressure applied together with the distinct particle packing might interpret the discrepancy observed for the optimal doses determined using CST and the present mechanical dewatering tests.

At the end of the consolidation, the axial load P was removed and the rebound of the sediment cake was observed over a period of 60,000 s. It was noted that the relaxation (rebound) of the sediment cake was restored with a time scale comparable with that of the consolidation processes, irrespective of the doses of the polyelectrolyte flocculation. However, the restored sediment thickness L_s was much thinner than the original thickness L_0. Within about 30,000 s, the relaxation/rebound was apparently related to the recoverable (elastic) deformation of the sediment cake, which constituted of about 20–30% of the total deformation. The remaining 70–80% was left as unrecoverable (plastic deformation). It was noted that the recovered cake is partly caused by the permeation of air into the consolidated cake and hence the saturation of water in the inter-particle pores was not unity after the rebound had occurred.

The dependence of transmitted pressure P_t on P for the original and flocculated sludge Sample-T is shown in Table 2. It is noted that the value of P_t/P increases with increasing axial load P from about 10% to 90% for all types of samples tested. This confirms the results shown in an earlier study such that the sidewall friction plays a key role in determining the consolidation dewatering behavior of a wet cake in a C–P cell (Wu et al., 2000).

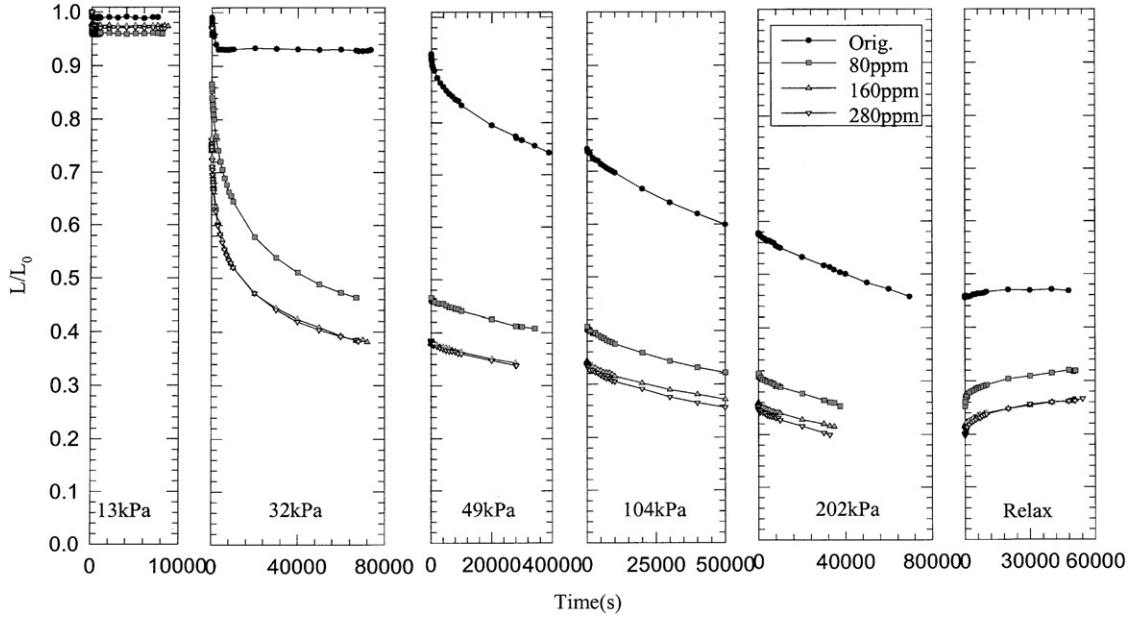

Fig. 4. Consolidation–relaxation curve for Testing Sample-T (with four different doses of original, 80, 160, and 280 ppm, respectively) on the T-cell. Five panels of L/L_0 vs. time curves are shown in the consolidation plot with increasing axial loads (in the order of 13, 32, 49, 104, and 202 kPa). Each plot is followed by a relaxation curve corresponding to the suddenly release of axial load, and then the cake thickness is recorded as a function of time.

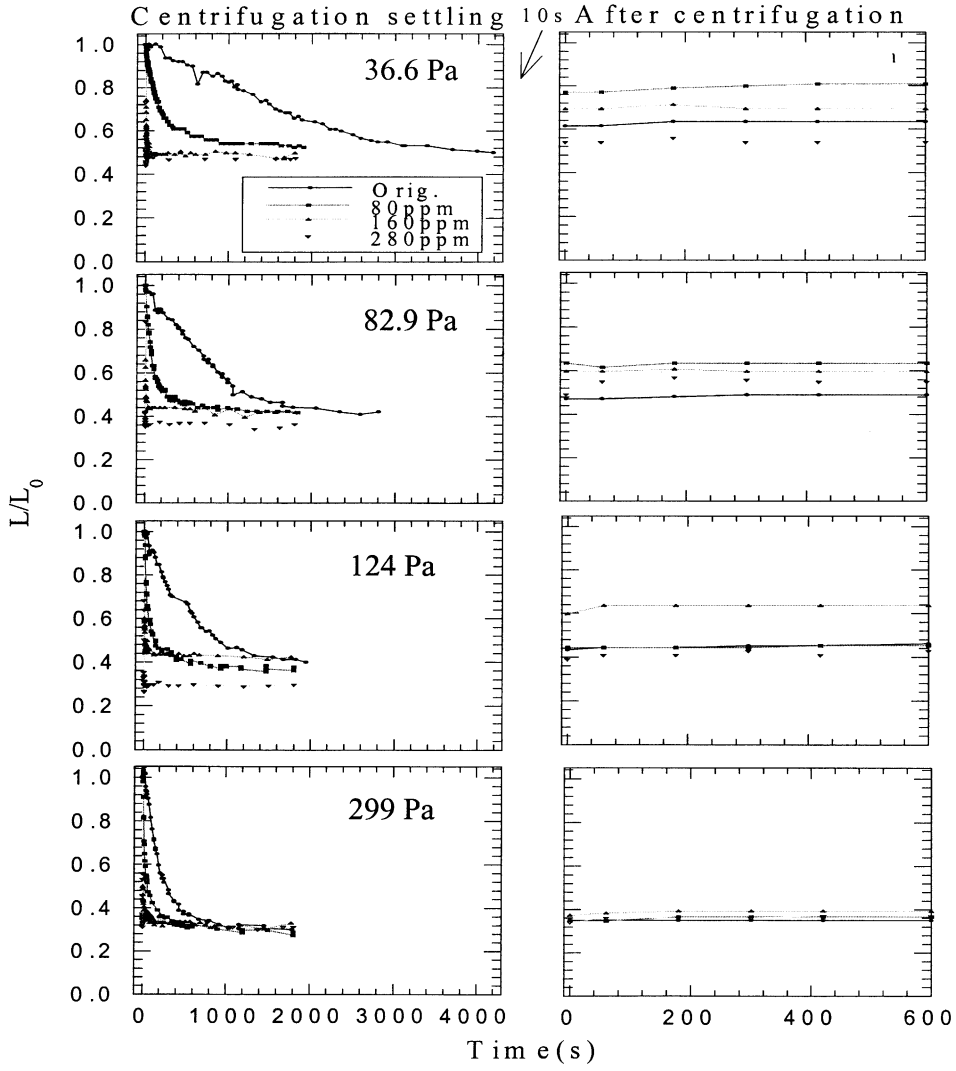

Fig. 5. Centrifugation-settling–relaxation curve for Testing Sample-T (with four different doses of original, 80, 160, and 280 ppm, respectively). Four panels of L/L_0 vs. time curves are shown in the consolidation plot with continuous increasing rotation speed (in the order of 300, 450, 550, 850 rpm). Each plot is followed by a relaxation curve in which the torque to the rotation is suddenly removed, and then the cake thickness is recorded as a function of time.

Using the same Sample-T, a series of centrifugal-setting-relaxation experiments were carried out and the results are shown in Fig. 5. It was noted that under an acceleration equivalent to the consolidation process, the sediment formation occurred within a much shorter time scale ranging from 1000 to 3000 s for the polyelectrolyte flocculated sludge and original sludge, respectively. It was interesting to observe that, similar to the case of consolidation dewatering, flocculated sludge reduced the time required for the sediment thickness L/L_0 to reach the value 0.3–0.5 as compared to the original sludge. The four rotational speeds had been calculated (Table 1) to correspond to the equivalent axial loads in the consolidation dewatering processes.

However, the resulting L/L_0 vs. time curves showed at least the following differences: (i) The final equilibrium sediment thickness was more dependent upon the polyelectrolyte doses in the consolidation dewatering processes. In contrast, its dependence was much weaker in the centrifugal setting experiments. This could be observed by noting nearly all samples achieved a similar equilibrium thickness L/L_0, irrespective of the polyelectrolyte doses. (ii) The rebound of the sediment thickness was achieved within a much shorter time scale, 200–600 s. This was in direct contrast with an extremely long relaxation time 30,000–60,000 s in consolidation dewatering experiments. The latter observation suggests that the structures of the packed cake after consolidation and centrifugal settling were very different. The last section provides some visual observations on the cake structure.

In order to understand the drastic difference in the dynamic pattern developed in consolidation dewatering/batch centrifugal-setting experiments, similar sets of experiments

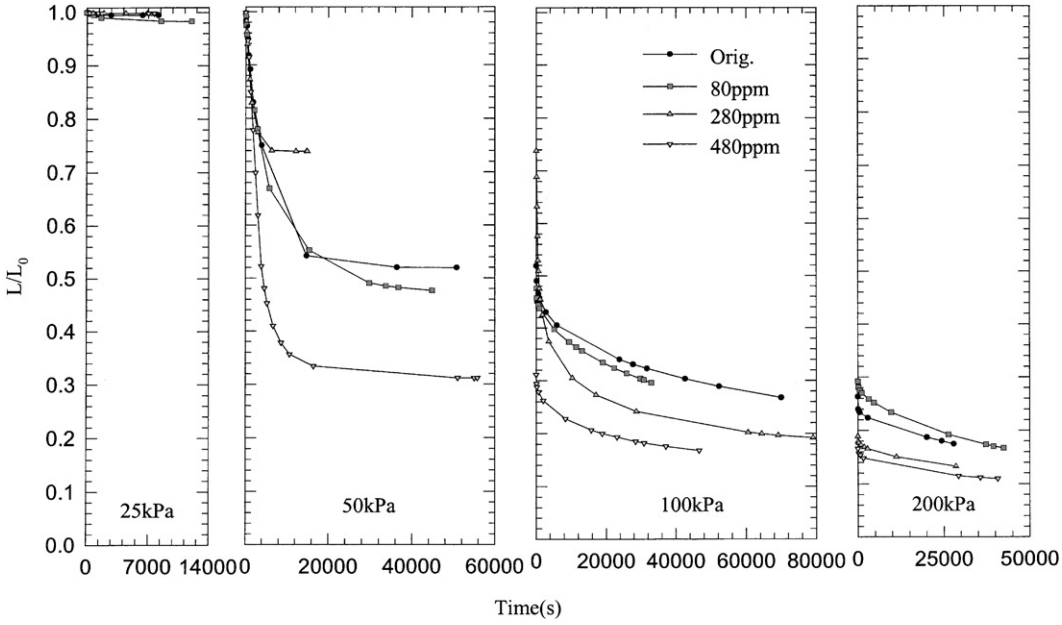

Fig. 6. Consolidation–relaxation curve for Testing Sample-U (with four different doses of original, 80, 280, and 480 ppm, respectively) on the S-cell. Four panels of L/L_0 vs. time curves are shown in the consolidation plot with increasing axial loads (in the order of 25, 50, 100, and 200 kPa).

were carried out on Sample-U, using CP cell-S, and continuous centrifugal setting experiments and the results for Sample-U were comparable. When $P = 25$ kPa, there was hardly any dewatering from the sediment cake (Fig. 6). When P exceeded 50 kPa, there was a significant collapse for the sludge sediment conditioned with a polyelectrolyte dose of 480 ppm. For lower doses of polyelectrolyte (original sludge, 80 and 280 ppm), the dewatering data contradicted with the CST estimated optimal dose 280 ppm as shown in Fig. 3. There was a reversal of dewatering capability for the lower dosed sludge samples at $P = 50$ kPa: the dewatering percentage for the three samples run in the decreasing order of the following sequence: 80 ppm, original sludge and 280 ppm with the sediment thickness L/L_0 (under the equilibrium stage) of 0.5, 0.54, and 0.74, respectively. The order for the dewatering percentage at equilibrium was changed at an even higher axial load P. At $P = 100$ and 200 kPa, the dewaterability of the original sludge and 80 ppm samples follows a similar trend as noted at 50 kPa.

To explain for the mismatch of CST-estimated optimal dose and consolidation dewatering tests, the Sample-U was subjected to another set of continuous centrifugal-settling/relaxation (rebound) experiments and the results are shown in Fig. 7. These sets of experiments differed from the Sample-T in the followings: (i) In order to compare data with consolidation dewatering tests, the same polyelectrolyte doses were used: original sludge, 80, 280, and 480 ppm. These turned out to be different from Sample-T. (ii) The centrifugal-settling experiments were carried out in a continuous mode with stepwise increases of rotational speed. This was in direct contrast with the Sample-T whose tests were done in a batch mode. At the rotational speed of 350 rpm (equivalent to acceleration $= 33.4g$), the sediment thickness for the sludge conditioned with polyelectrolyte at the doses 80 and 480 ppm was significantly reduced. The equilibrium thickness L/L_0 for 80 and 480 ppm samples was measured as 0.85 and 0.65, respectively. In contrast, the equilibrium L/L_0 values of the original sludge and 280 ppm samples were close to 0.95, not too far away from the original sediment height.

3.1. Yield stress

Theoretical estimation of the null-stress solids fraction ϕ_g (gelling point) and the yield stress $P_y(\phi)$ were conducted by the following procedures. The relationship between normal stress and average solids fraction in the sediment controls the dewatering rate of the sediment. The normal stress on the supernatant/sediment interface in the centrifuge could be approximated as follows:

$$P = \int_{R-H_0}^{R-H} \left(\frac{\partial p_L}{\partial r}\right) \mathrm{d}r = \int_{R-H_0}^{R-H} (\rho_L \Omega^2 r)\, \mathrm{d}r$$

$$= \frac{\Omega^2 \rho_L}{2}[(R-H)^2 - (R-H_0)^2]. \quad (8)$$

Fig. 8 depicts the curves of normal stress P vs. average solids fraction in the sediment ϕ for Sample-U and Sample-T sludge, respectively, with flocculent doses as the parameter. The dashed line in the figures represented the original solids fraction of sludge ϕ_0. Slopes of the ϕ_S–P_S curves could be taken as an index to characterize the sediment compactibility. The intercept on the x-axis ($P=0$) was the corresponding ϕ_g of the sludge. For Sample-U, ϕ_g for sludges flocculated

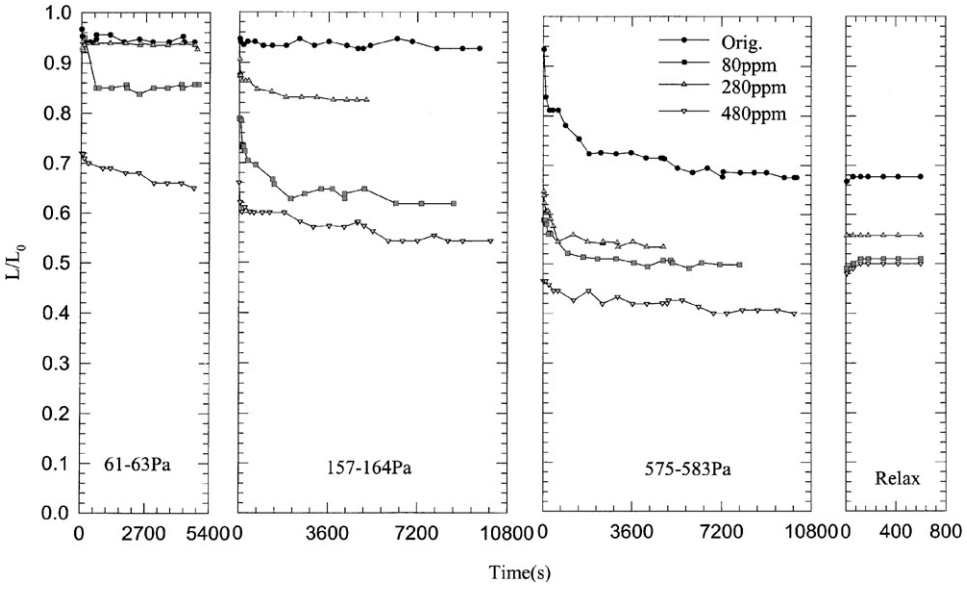

Fig. 7. Centrifugation-settling–relaxation curve for Testing Sample-U (with four different doses of original, 80, 280, and 480 ppm, respectively). Three panels of L/L_0 vs. time curves are shown in the consolidation plot with continuous increasing rotation speed (in the order of 350, 560, 1050 rpm). This is followed by a relaxation plot in which the torque to the rotation is suddenly removed, and then the cake thickness is recorded as a function of time.

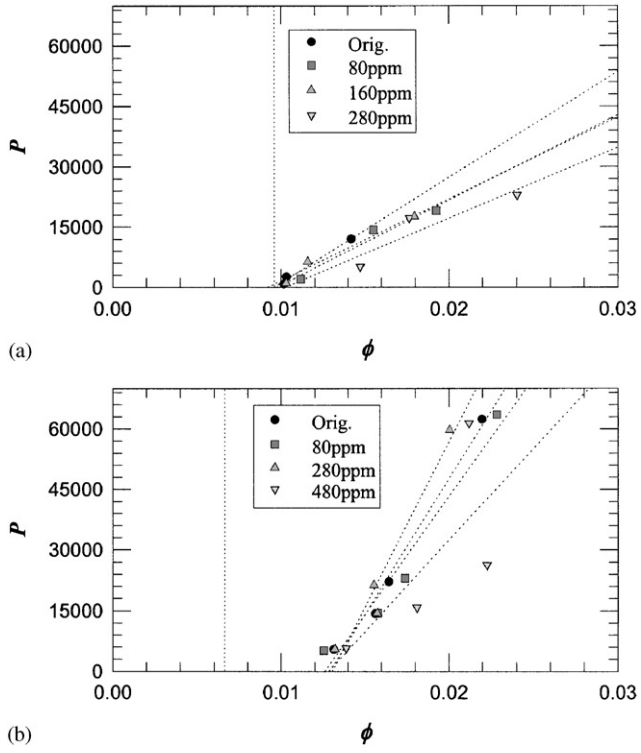

Fig. 8. ϕ_g evaluation from P vs. ϕ curve: (a) for Sample-U sludge, circle: 0 ppm; square: 80 ppm; triangle: 280 ppm; and inverse triangle: 480 ppm and (b) for Sample-T sludge, circle: 0 ppm; square: 80 ppm; triangle: 160 ppm; and inverse triangle: 280 ppm.

at all doses converged at 0.009, which almost coincided with ϕ_0. All flocs in the initial suspension are in physical contact with each other and form a network matrix. While being subject to the subsequent centrifugal compaction, the sediment readily yielded from 0.009 to 0.025, corresponding to the elevation of pressure to around 25,000 Pa. In comparison with the Sample-U, Sample-T sludge exhibited stiffer sediment with a higher ϕ_g (nearly 0.013 for sludge conditioned at all doses) and less compactible behavior. To achieve the same solids fraction, the required pressure (up to 63,000 Pa) is two times higher than Sample-U sludge. While considering the effects of flocculation, though no apparent effects occurred on the ϕ_g, the compatibility and achievable final solids fraction increased with the flocculent doses. Overdosing caused no deterioration on the dewaterability.

Many filtration-related works had proposed different ways to estimate the yield stress P_y, which is essential to reveal the deformation behavior of sediment or cake. To evaluate the yield stress, herein we followed Buscall and White's method (Buscall & White, 1987) to calculate the estimated yield stress and solids fraction at the centrifugal filter cell bottom ($z = 0$ defined in this reference). They assumed a relationship $P \propto (\phi - \phi_g)^m$ for initial guess to obtain the P_y vs. ϕ correlation according to the following equations:

$$P_y \cong P(0) \cong \Delta\rho\, g \phi_0 H_0 \left(1 - \frac{H_{eq}}{2R}\right), \tag{9}$$

$$\phi(0) = \frac{\phi_0 H_0 \left[1 - \frac{1}{2R}(H_{eq} + g\frac{dH_{eq}}{dg})\right]}{\left[(H_{eq} + g\frac{dH_{eq}}{dg})(1 - \frac{H_{eq}}{R}) + \frac{H_{eq}^2}{2R}\right]}, \tag{10}$$

where H_{eq} is the equilibrium sediment height, R is the radius of rotation for the centrifugal process. From Fig. 9, the range of m for Sample-T and -U is between 1 and 2.

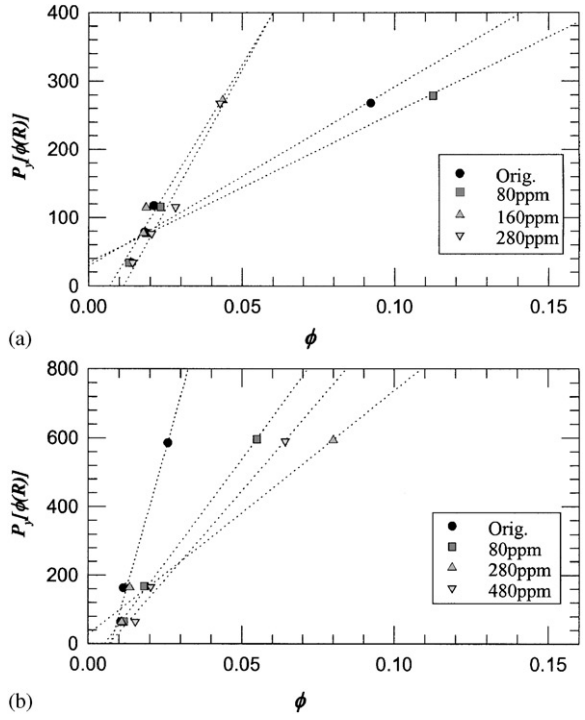

Fig. 9. The relation between the yield stress and volume fraction based on centrifugal-settling test: (a) Sample-T and (b) Sample-U. P_y vs. ϕ curves according to Eqs. (9) and (10).

The error involved in using Eqs. (9) and (10) between $m=1$ and 2 is below ca. 10%. Except for some data points at high P_y, all the regression lines had the same intercepts on the X-axis, which were 0.006 for Sample-U and 0.01 for Sample-T. These two solids fractions, denoted as $\phi_{g,y}$, could be viewed as a threshold value for yielding. Noticeably, $\phi_{g,y}$ of Sample-U is lower than its ϕ_0, and in contrast, the one of Sample-T is higher. A stiffer sediment matrix formed in the Sample-T sludge might be resulted from this. Similar to the situation described in Fig. 8, flocculation would enhance the yielding under the same stress, at which the enhancement is more significant in the case of Sample-T sludge.

However, such an observation deviates significantly from the results of C–P cell, as the sludge required a much higher stress for significant yield (50,000 Pa for Sample-U and 30,000 Pa for Sample-T). P_y may be an operational definition and vary according to the measuring methods. The comparison of P_y from different methods is hardly possible.

3.2. Structure and dewatering dynamics for the wet cake formed by consolidation and centrifugal setting

Observations have been made from the surface pictures taken from the equilibrium cakes formed via consolidation dewatering and centrifugal sedimentation, respectively, under different pressure gradients. The calculated values of dP/dx are in general in the same order of magnitude with dP/dr (Tables 1 and 2). This seems to be in direct contrast with the observation such that the dewatering time scale required by centrifugal sedimentation is about one order of magnitude smaller than the consolidation dewatering. It is seen that the cake formed by consolidation has a more compact structure (Fig. 10).

To further elucidate this problem, we took the scanning electron microscopic photos of the sludge surface morphology prior to dewatering and after centrifugation and consolidation (Fig. 10). The observing position was at the piston/cake interface for consolidated sludge and sediment/air interface for centrifugal settled cake. The magnification was set as 1000. In the case of original sludge, the single floc is highly porous and lots of the filament could be noticed. The cake obtained from dewatering had more compact appearance. After centrifugal settling, the flocs looked shrunk and were stacked closely with each other (Fig. 10c). Further consolidation deteriorated the intrinsic porous structure and flatten appearance was observed (Fig. 10e). In the case of flocculated sludge, in contrast to the original sludge flocs, a compact and layer-by-layer structure was noticed. After the centrifugation, however, this structure seemed to be disrupted first and then re-stacked. Consolidation also caused to flatten and compress cake surfaces, but with a relatively porous morphology (comparing with the original sludge cake). To qualitatively describe the term "porosity", we processed the image analysis tests on these SEM pictures by the function "*blob analysis*" in the commercial software *Inspector* (Matrox), to obtain the two-dimensional projected porosity and equivalent pore size $d_p(=\sqrt{4A_p/\pi}$, of those dark and concave portions, where A_p is the projected area of the pore). The porosity is defined as the portion of projected area of inter-aggregate space, which might not include the moisture contained in the floc/aggregates (surface water or chemically bound water). The results are listed in Table 3. In considering the effects of pressure on the cake structure, the porosity decreased from 0.369 for a single floc to 0.349 for centrifugal settled cake and to 0.258 for the compressed cake of original sludge. Similar trends were also noticed in the case of flocculated sludge, from 0.469 for a single floc to 0.434 for centrifugal cake and to 0.414 for compressed cake. This could be realized by the fact that in general the equilibrium solid pressure in the consolidation dewatering (P_m: 4–200 and 7–173 kPa for the Sample-T and Sample-S, respectively) is 1–2 orders of magnitude higher than the centrifugal sedimentation (P_s: 36–300 and 60–600 Pa for the cell-T and cell-S, respectively). While considering the effects of flocculation, the flocculated ones were always with a higher porosity than those of original sludges. In contrast to the common experiences, the porosity of consolidated flocculated sludge cake (0.414) was even higher than the original sludge floc (0.369). The pore sizes of the sludge before and after dewatering were pretty similar (around 2 μm), but significant changes were found in the standard deviation of pore sizes, where the deviation was generally decreased with increasing pressure.

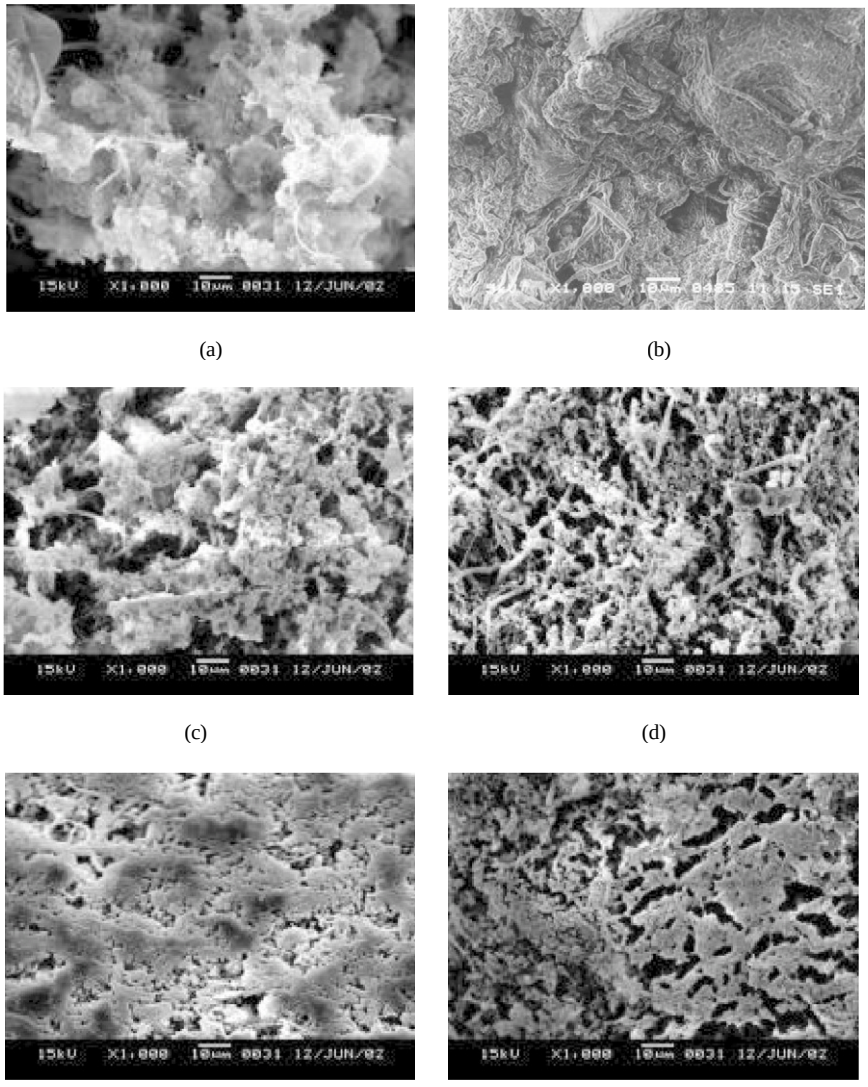

Fig. 10. Sediment/cake surface structure formed under centrifugal settling and consolidation dewatering: (a) Original sludge floc; (b) flocculated sludge floc; (c) centrifugal sludge cake (original); (d) centrifugal sludge cake (flocculated); (e) consolidated sludge cake (original); and (f) consolidated sludge cake (flocculated).

Table 3
Surface structure of the sediment/cake formed in consolidation dewatering and centrifugal-settling experiments

	Fig. 10a	Fig. 10b	Fig. 10c	Fig. 10d	Fig. 10e	Fig. 10f
Porosity	0.369	0.469	0.349	0.433	0.258	0.414
Pore size (μm)	0.956	1.25	1.06	0.914	0.901	0.899
Standard deviation	2.00	2.80	2.08	1.81	1.16	1.70

Referring to Figs. 4 and 5, the consolidation time scale is much longer than the centrifugal sedimentation. This could be explained by the higher resistance offered to water flow throughout the cake due to the more compact structure achieved by consolidation.

Using scale analysis, Landman and Russel (1993) compared the filtration and sedimentation time scales for concentrated suspensions. They found that the ratio of the time scale is given by

$$\frac{T_{\text{Filtration}}}{T_{\text{Sedimentation}}} \approx \frac{\Delta\rho\, g\phi_0 l_0}{\sigma}\,\frac{V(\phi_0)}{V(\phi_b)}, \tag{11}$$

where $V(\varphi)$ and σ refer to the sedimentation velocity and constant pressure drop, respectively. φ_0 and φ_b refer to

the volume fraction of solids at the supernatant and sediment/cake, respectively.

One of the underlying assumptions used here is that filtration properties could be determined by compression–permeation tests in a C–P cell and hence the filtration time scale is comparable with the consolidation dewatering process. Furthermore, the sedimentation process is governed by the magnitude of gravitational acceleration. Looking at the following two limiting cases considered by Landman and Russel (1993): (i) When the solid fraction is close to the random close packing volume fraction, the filtration time scale is comparable to or larger than the sedimentation time scale. (ii) When low to moderate pressure difference and φ_b is of the order of 0.2, the filtration time is three orders of magnitude smaller than the gravitation settling time.

From Table 1, the centrifugal acceleration Γ $(=r\Omega^2/g)$ and solidosity ε_s are in the range $\Gamma = 26$–330 and 0.01–0.02, respectively. Taking the filtration time scale to be comparable to the consolidation dewatering time scale, $T_{\text{Filtration}} \sim T_{\text{Consolidation}}$. Suppose the time scales of centrifugal settling is related to the gravity sedimentation by the following:

$$\frac{T_\Gamma}{T_{\text{Sedimentation}}} \approx \frac{1}{\Gamma}. \tag{12}$$

By Eqs. (11) and (12), the following time scale ratio is readily available:

$$\frac{T_{\text{Consolidation}}}{T_\Gamma} \approx \frac{\Delta\rho\, g\phi_0 l_0}{\sigma}\,\frac{V(\phi_0)}{V(\phi_b)}\Gamma. \tag{13}$$

Following Landman and Russel (1993), the parameter σ is scaled with the yield stress P_y. The data of the centrifuge experiments are processed with the method reported by Buscall and White (1987) and Chu, Ju, Lee, and Mohanty (2002). The results show that the yield stress of the activated sludge Sample-T is of the order of 10–100 Pa. For instance, in Sample-T, the parameter values for $\Delta\rho$, φ_0, l_0 are 450 kg/m^3, 0.00655, and 0.05 m, respectively. Since φ_b $(=0.01-0.02) \sim \varphi_0$ (0.0065), the ratio $V(\varphi_b)/V(\varphi_0) \sim$ O(1). Taking these all into account it is seen from Eq. (13) that

$$\frac{T_{\text{Consolidation}}}{T_\Gamma} \approx \frac{\Delta\rho\, g\phi_0 l_0}{\sigma}\,\frac{V(\phi_0)}{V(\phi_b)}\Gamma \approx 0.144\Gamma \approx 4-18. \tag{14}$$

From Eq. (14), it is estimated that the consolidation (filtration) time scale is one order of magnitude higher than the sedimentation time scale. Hence, the experimentally determined dynamic time scale agrees reasonably well with the theory by Landman and Russel (1993).

4. Conclusions

This work has reviewed the similarity and difference between the consolidation dewatering and centrifugal sedimentation processes. Both processes showed qualitatively similar features for the optimal dose of flocculation. The dewatering rate of the consolidation processes was one order of magnitude lower than the centrifugal sedimentation although both processes reach roughly the same equilibrium cake thickness and moisture contents. The difference in the moisture removal rate is discussed and the results matched reasonably well with the theory of Landman and Russel (1993). The continuous and batch operation of centrifugal sedimentation did not introduce significant difference in the moisture removal rate and equilibrium sediment/cake thickness. The rebound of cake was observed for both processes when the external driving forces (axial load and rotation torque) were removed although the mechanism for such behavior was different for the two processes.

Acknowledgements

We would like to acknowledge the National Science Council (Taiwan) for the support under the Grant Number NSC 89-2214-E-002-058. CHW thanks the National Taiwan University for the visiting appointment during January–May 2002.

References

Buscall, R., & White, L. R. (1987). On the consolidation of concentrated suspension. I: The theory of sedimentation. *Journal of Chemical Society, Faraday Transaction I*, *83*, 873–891.

Christensen, J. R., Sorensen, P. B., Christensen, G. L., & Hansen, J. A. (1993). Mechanisms for overdosing in sludge conditioning. *Journal of Environmental Engineering*, *119*, 159–171.

Chu, C. P., Ju, S. P., Lee, D. J., & Mohanty, K. K. (2002). Batch gravitational sedimentation of slurries. *Journal of Colloid and Interface Science*, *245*, 178–186.

Chu, C. P., & Lee, D. J. (2001). Experimental analysis of centrifugal dewatering process of polyelectrolyte flocculated waste activated sludge. *Water Research*, *35*, 2377–2384.

de Kretser, G., Shane, S. P., Scales, P. J., Boger, D. V., & Landman, K. A. (2001). Rapid filtration measurement of dewatering design and optimization parameters. *AIChE Journal*, *47*, 1758–1769.

Landman, K. A., & Russel, W. B. (1993). Filtration at large pressure for strongly flocculated suspensions. *Physics of Fluids A*, *5*, 550–560.

Landman, K. A., White, L. R., & Eberl, M. (1995). Pressure filtration of flocculated suspensions. *AIChE Journal*, *41*, 1687–1700.

Lee, D. J. (1994). Measurement of bound water in waste activated sludge: Use of the centrifugal setting method. *Journal of Chemical Technology and Biotechnology*, *61*, 139–144.

Lee, D. J., & Hsu, Y. H. (1992). Fluid flow in capillary suction apparatus. *Industrial & Engineering Chemistry Research*, *31*, 2379–2384.

Lee, D. J., & Hsu, Y. H. (1993). Cake formation in capillary suction apparatus. *Industrial & Engineering Chemistry Research*, *32*, 1180–1185.

Lin, W. W., & Lee, D. J. (2001). Liquid saturation profile in capillary suction time filter paper fluid flow in capillary suction apparatus. *Industrial & Engineering Chemistry Research*, *40*, 808–813.

Lu, W. M., Huang, Y. P., & Hwang, K. J. (1998). Stress distribution in a confined wet cake in the compression–permeability cell and its application. *Powder Technology*, *97*, 16–25.

Murase, T., Iwata, M., Adachi, T., Gmachowski, L., & Shirato, M. (1989). An evaluation of compression–permeability characteristic in the intermediate concentration range by use of centrifugal and constant-rate compression techniques. *Journal of Chemical Engineering of Japan*, *22*, 378–381.

Teoh, S. K., Tan, R. B. H., He, D., & Tien, C. (2001). A multifunction test cell for cake filtration studies. *Transaction of Filtration Society*, *1*, 81–90.

Usher, S. P., de Kretser, R. G., & Scales, P. J. (2001). Validation of a new filtration technique for dewatering characterization. *AIChE Journal*, *47*, 1561–1570.

Wu, R. M., Lee, D. J., Wang, C. H., Chen, J. P., & Tan, R. B. H. (2001). Novel cake characteristics of waste-activated sludge. *Water Research*, *35*, 1358–1362.

Wu, R. M., Lee, D. J., Zhao, J., Wang, C. H., & Tan, R. B. H. (2000). Discrepancy in cake characteristic measurement: Compression–permeability cell. *Journal of Chemical Engineering of Japan*, *33*, 869–878.

Yen, P. S., & Lee, D. J. (2001). Errors in bound water measurements using centrifugal setting method. *Water Research*, *35*, 4004–4009.